



CentraleSupélec



LISTIC

Change Detection for SAR Images in non-Gaussian Environment

Ammar Mian

10 July 2018

CentraleSupélec SONDRA, LISTIC

Plan of the presentation

Introduction and Problematic

Change Detection Overview

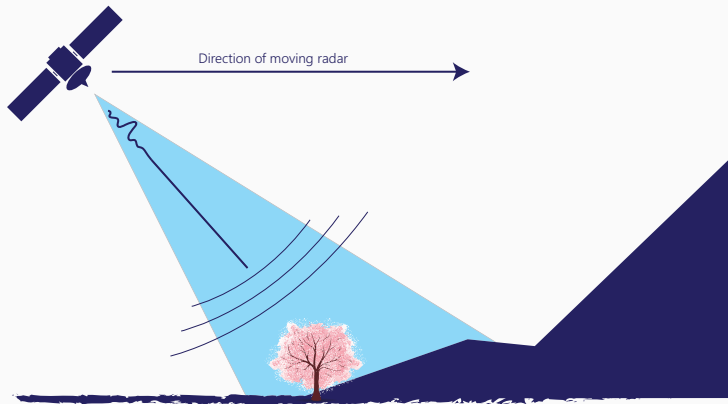
Change Detection in non-Gaussian Context

Introduction and Problematic

Synthetic Aperture Radar

Synthethic Aperture Radar (SAR) images allow to observe a scene of interest over time.

- All weather/illumination imaging capabilities
- See objects in radar band of frequencies (P, L, X)



Change Detection

Recent years have seen a **huge** increase in the number of images (Sentinel-1, TerraSAR-X, UAVSAR, etc). Change Detection in those images is useful for applications such as:

- Activity monitoring:



Change Detection

Recent years have seen a **huge** increase in the number of images (Sentinel-1, TerraSAR-X, UAVSAR, etc). Change Detection in those images is useful for applications such as:

- Activity monitoring:



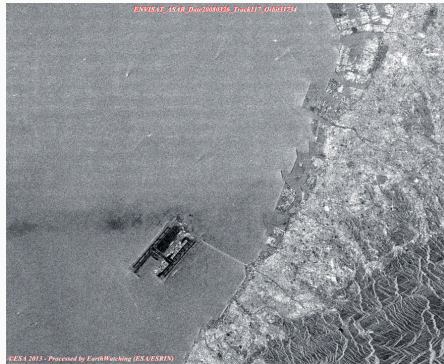
ERS-2 SAR Date 20010919 Track 117 Orbit 33330

©ESR 2011 - Processed by EarthWatching (ESR/PSRIN)

Change Detection

Recent years have seen a **huge** increase in the number of images (Sentinel-1, TerraSAR-X, UAVSAR, etc). Change Detection in those images is useful for applications such as:

- Activity monitoring:



Introduction

Recent years have seen a **huge** increase in the number of images (Sentinel-1, TerraSAR-X, UAVSAR, etc). Change Detection in those images is useful for applications such as:

- Damage assessment:



Introduction

Recent years have seen a **huge** increase in the number of images (Sentinel-1, TerraSAR-X, UAVSAR, etc). Change Detection in those images is useful for applications such as:

- Damage assessment:



Problematics

Sometime the images available are **multivariate**:

- PolSAR: backscattering in different modes of polarisation
- InSAR: backscattering when scene is seen through two closes angles
- Spectro-angular information: backscattering seen through different frequencies and looking angles. (See. [Mian et al., 2017, Mian et al., 2018b])

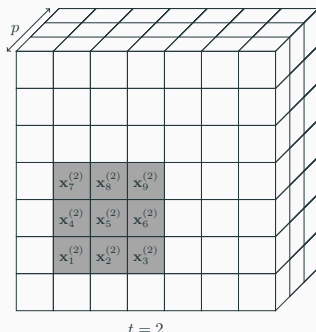
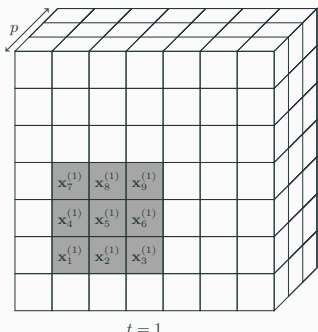
Objectives

- Reliable automatic Unsupervised Change Detection.
- Taking into account the nature of the data (High-resolution and **Multivariate**).

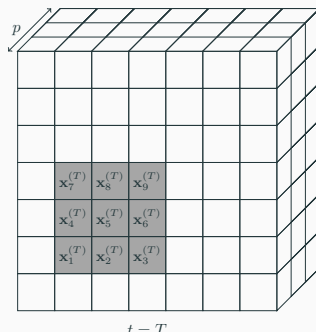
Change Detection Overview

Some definitions

Illustration of local data ($N = 9$, $p = 3$). The central pixel ($\mathbf{x}_5^{(t)}$) is the test pixel.



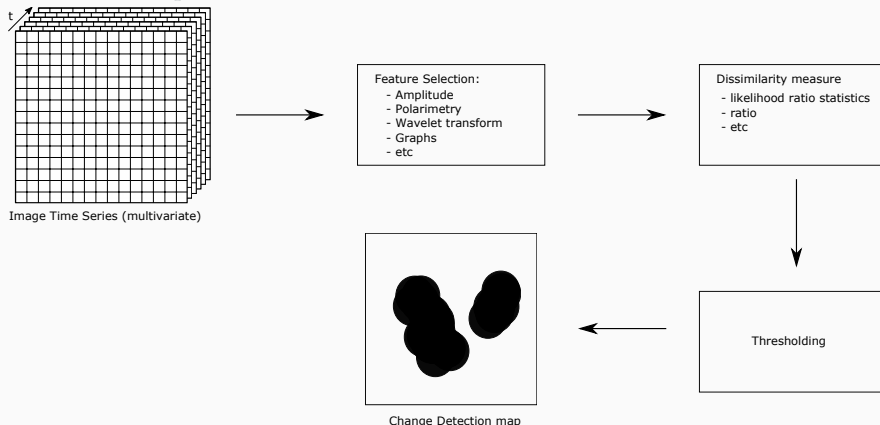
...



Unsupervised Change Detection Framework

Two kind of approaches [Hussain et al., 2013]:

- Object based techniques.
- Pixels-based techniques:



Background on statistics for Change Detection

Method	Description	Cons	Pros
[Novak, 2005b] [Preiss and Stacy, 2008]	Compute cross-correlations between two dates	bi-date need phase coherence threshold	No model
[Ratha et al., 2017] [Nascimento et al., 2018]	Use information theory to compute a distance between two dates	bi-date Model Assumption	threshold
[Conradsen et al., 2001] [Novak, 2005a]	Test of equality between covariance matrices at each date	Gaussian assumption	multi-dates Threshold

Hypothesis testing

Observations are independent and we have $\mathbf{x}_k^{(t)} \sim p_{\mathbf{x}}(\mathbf{x}; \boldsymbol{\Omega}_t)$, where $\boldsymbol{\Omega}_t \in \boldsymbol{\Theta}$ are the parameters of the Probability Distribution Function (PDF).

The Detection Problem

Decide between:

$$\begin{cases} H_0 : \boldsymbol{\theta}_1 = \dots = \boldsymbol{\theta}_T = \boldsymbol{\theta}_0, \\ H_1 : \exists (t, t') \in [1, T]^2, \boldsymbol{\theta}_t \neq \boldsymbol{\theta}_{t'} \end{cases},$$

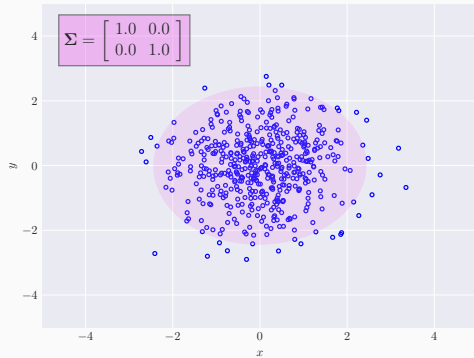
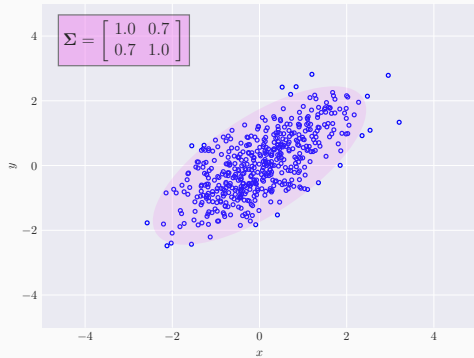
where $\boldsymbol{\theta}_t \subset \boldsymbol{\Omega}_t$ are the parameters of interest.

Classically for SAR images $\boldsymbol{\theta}_t = \{\boldsymbol{\Sigma}_t\}$ with $\boldsymbol{\Sigma}_t$ parameter of the PDF:

$$p_{\mathbf{x}}^{\mathcal{CN}}(\mathbf{x}; \mathbf{0}_p, \boldsymbol{\Sigma}_t) = \frac{1}{\pi^p |\boldsymbol{\Sigma}|} \exp(-\mathbf{x}^H \boldsymbol{\Sigma}_t^{-1} \mathbf{x}).$$

We define $\boldsymbol{\Phi}_t = \boldsymbol{\Omega}_t \setminus \boldsymbol{\theta}_t$.

Illustration case $p = 2$



Statistics of decision under Gaussian model

Many statistic exists (see [Ciuonzo et al., 2017]). The most popular is:

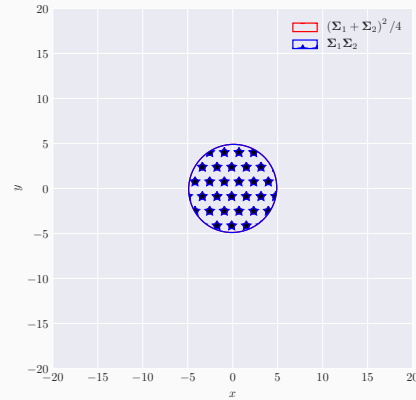
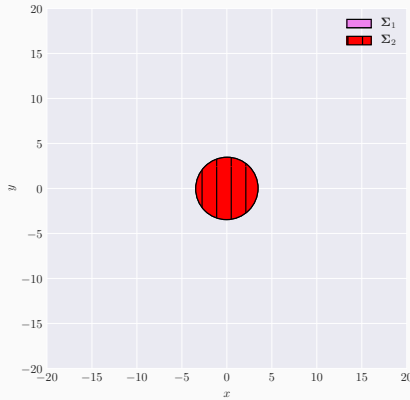
$$\hat{\Lambda}_G = \frac{\left| \hat{\Sigma}_0^{\text{SCM}} \right|^{TN}}{\prod_{t=1}^T \left| \hat{\Sigma}_t^{\text{SCM}} \right|^N} \stackrel{H_1}{\gtrless} \stackrel{H_0}{\lesssim} \lambda, \quad \forall t, \hat{\Sigma}_t^{\text{SCM}} = \frac{1}{N} \sum_{k=1}^N \mathbf{x}_k^{(t)} \mathbf{x}_k^{(t)H}, \hat{\Sigma}_0^{\text{SCM}} = \frac{1}{T} \sum_{t=1}^T \hat{\Sigma}_t^{\text{SCM}},$$

Properties

The statistic $\hat{\Lambda}_G$ is CFAR matrix. We have:

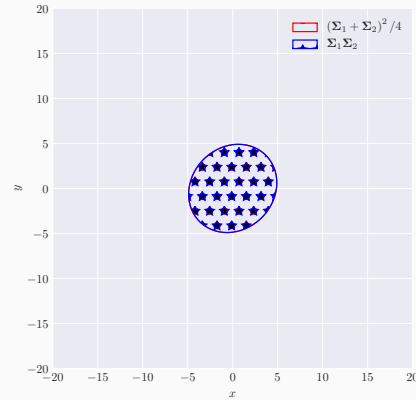
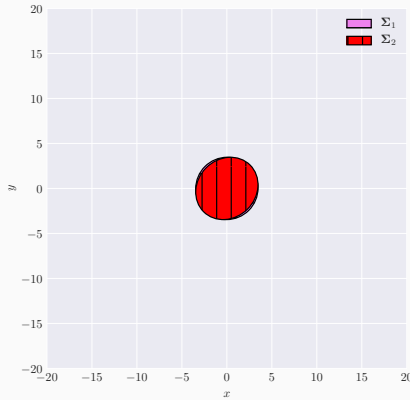
$$P \left\{ 2\rho \log(\hat{\Lambda}_G) \leq z \right\} \approx P \left\{ \chi^2(f^2) \leq z \right\} + \omega_2 \left[P \left\{ \chi^2(f^2 + 4) \leq z \right\} - P \left\{ \chi^2(f^2) \leq z \right\} \right]$$
$$f = (T-1)p^2, \rho = 1 - \frac{(2p^2-1)}{6(T-1)p} \left(\frac{T}{N} - \frac{1}{NT} \right),$$
$$\omega_2 = \frac{p^2(p^2-1)}{24\rho^2} \left(\frac{T}{N^2} - \frac{1}{(NT)^2} \right) - \frac{p^2(T-1)}{4} \left(1 - \frac{1}{\rho} \right)^2$$

Visualisation of Test: variation of shape



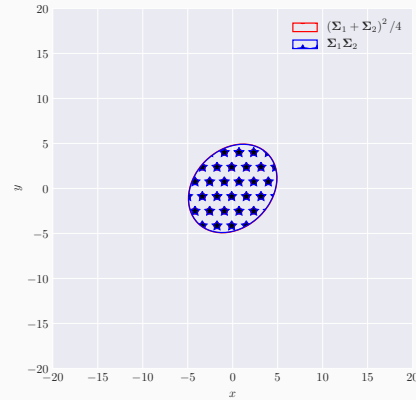
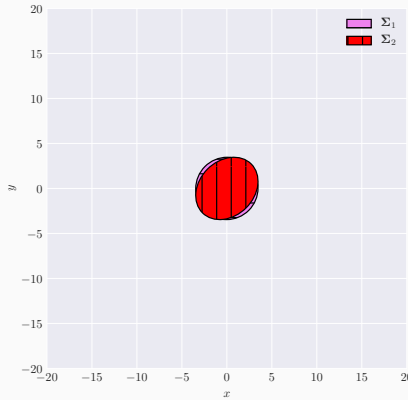
$$\Sigma_1 = \begin{bmatrix} 1 & 0.01 \\ 0.01 & 1 \end{bmatrix} \quad \Sigma_2 = \begin{bmatrix} 1 & 0.01 \\ 0.01 & 1 \end{bmatrix}$$

Visualisation of Test: variation of shape



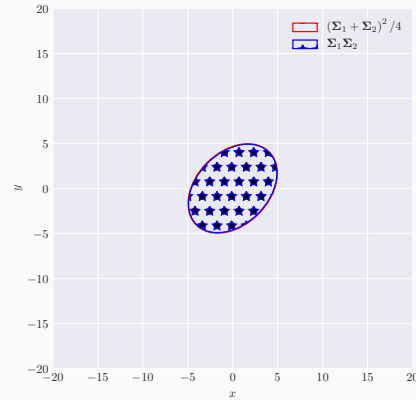
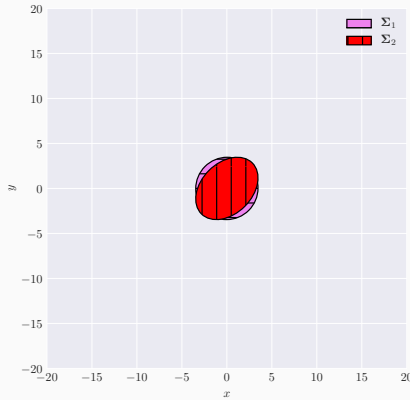
$$\Sigma_1 = \begin{bmatrix} 1 & 0.01 \\ 0.01 & 1 \end{bmatrix} \quad \Sigma_2 = \begin{bmatrix} 1 & 0.12 \\ 0.12 & 1 \end{bmatrix}$$

Visualisation of Test: variation of shape



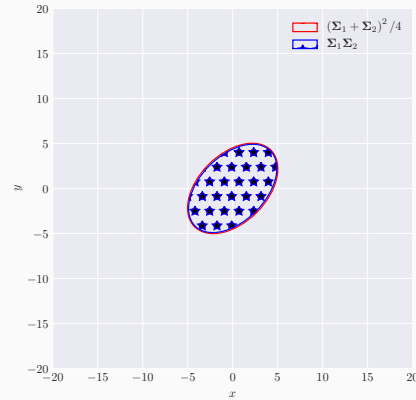
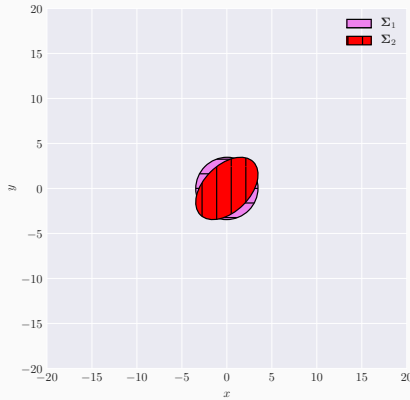
$$\Sigma_1 = \begin{bmatrix} 1 & 0.01 \\ 0.01 & 1 \end{bmatrix} \quad \Sigma_2 = \begin{bmatrix} 1 & 0.23 \\ 0.23 & 1 \end{bmatrix}$$

Visualisation of Test: variation of shape



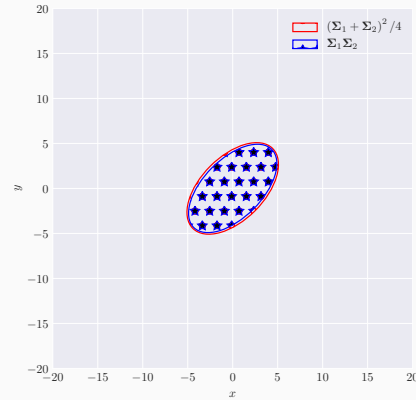
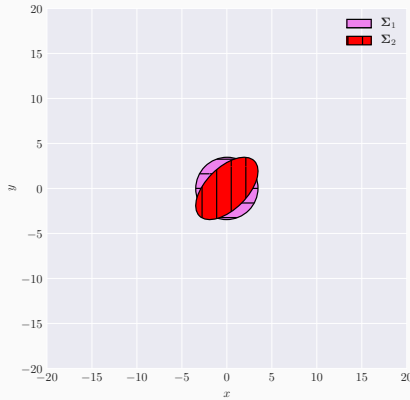
$$\Sigma_1 = \begin{bmatrix} 1 & 0.01 \\ 0.01 & 1 \end{bmatrix} \quad \Sigma_2 = \begin{bmatrix} 1 & 0.34 \\ 0.34 & 1 \end{bmatrix}$$

Visualisation of Test: variation of shape



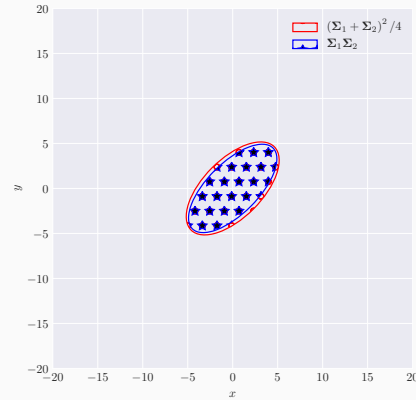
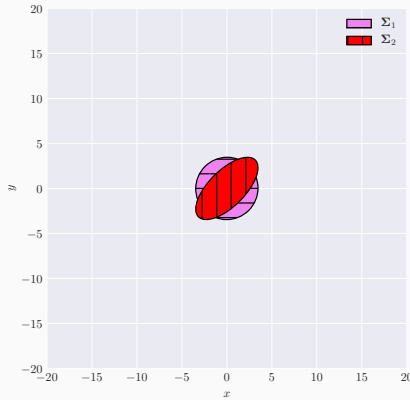
$$\Sigma_1 = \begin{bmatrix} 1 & 0.01 \\ 0.01 & 1 \end{bmatrix} \quad \Sigma_2 = \begin{bmatrix} 1 & 0.45 \\ 0.45 & 1 \end{bmatrix}$$

Visualisation of Test: variation of shape



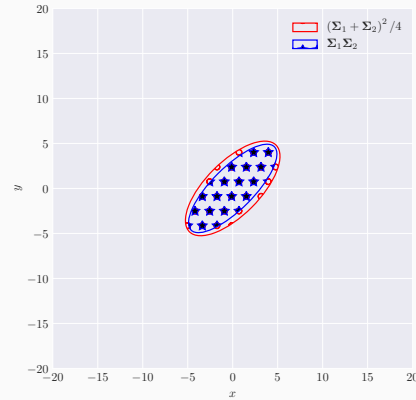
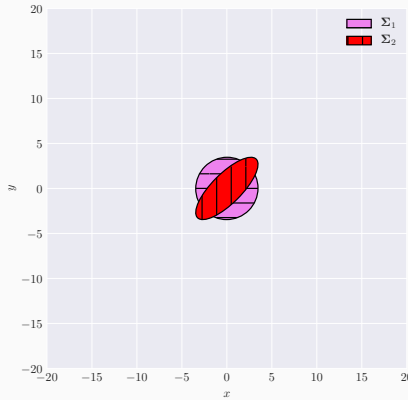
$$\Sigma_1 = \begin{bmatrix} 1 & 0.01 \\ 0.01 & 1 \end{bmatrix} \quad \Sigma_2 = \begin{bmatrix} 1 & 0.55 \\ 0.55 & 1 \end{bmatrix}$$

Visualisation of Test: variation of shape



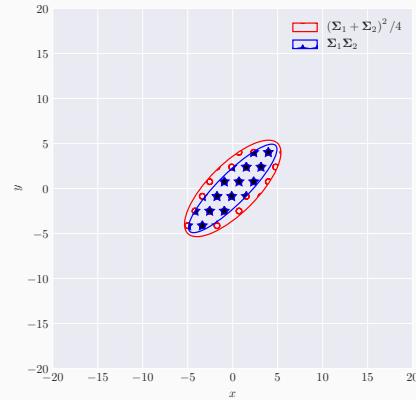
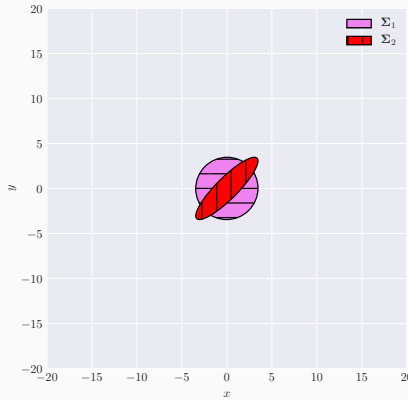
$$\Sigma_1 = \begin{bmatrix} 1 & 0.01 \\ 0.01 & 1 \end{bmatrix} \quad \Sigma_2 = \begin{bmatrix} 1 & 0.66 \\ 0.66 & 1 \end{bmatrix}$$

Visualisation of Test: variation of shape



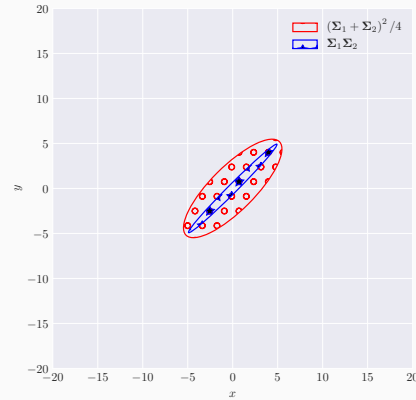
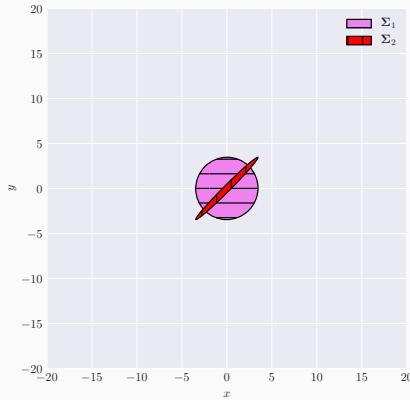
$$\Sigma_1 = \begin{bmatrix} 1 & 0.01 \\ 0.01 & 1 \end{bmatrix} \quad \Sigma_2 = \begin{bmatrix} 1 & 0.77 \\ 0.77 & 1 \end{bmatrix}$$

Visualisation of Test: variation of shape



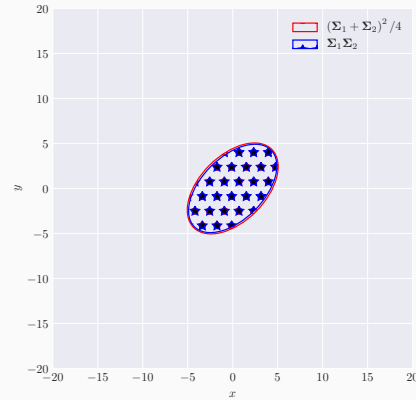
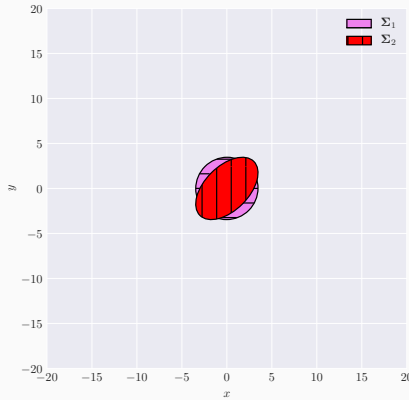
$$\Sigma_1 = \begin{bmatrix} 1 & 0.01 \\ 0.01 & 1 \end{bmatrix} \quad \Sigma_2 = \begin{bmatrix} 1 & 0.88 \\ 0.88 & 1 \end{bmatrix}$$

Visualisation of Test: variation of shape



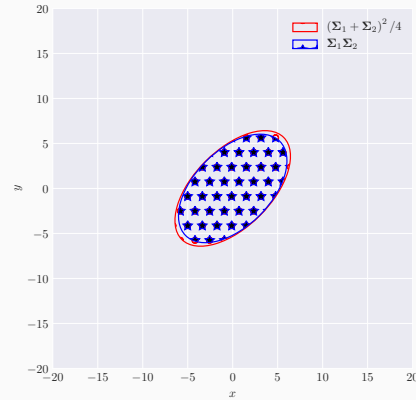
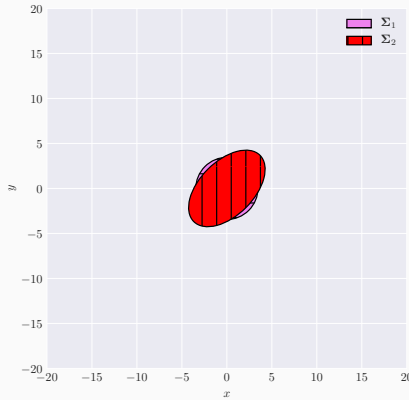
$$\Sigma_1 = \begin{bmatrix} 1 & 0.01 \\ 0.01 & 1 \end{bmatrix} \quad \Sigma_2 = \begin{bmatrix} 1 & 0.99 \\ 0.99 & 1 \end{bmatrix}$$

Visualisation of Test: variation of scale



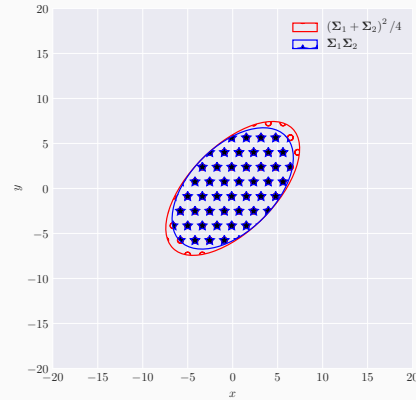
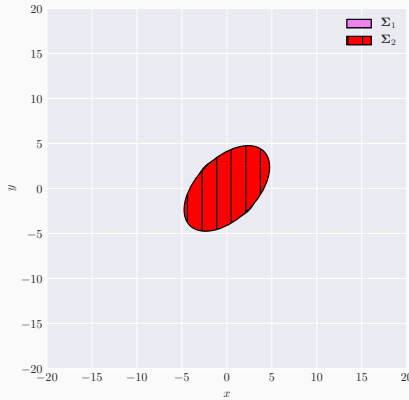
$$\Sigma_1 = \begin{bmatrix} 1 & 0.50 \\ 0.50 & 1 \end{bmatrix} \quad \Sigma_2 = 1.0 \times \begin{bmatrix} 1 & 0.50 \\ 0.50 & 1 \end{bmatrix}$$

Visualisation of Test: variation of scale



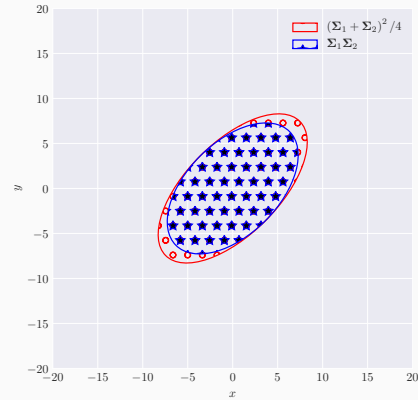
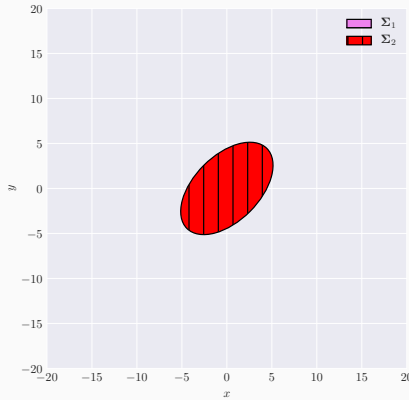
$$\Sigma_1 = \begin{bmatrix} 1 & 0.50 \\ 0.50 & 1 \end{bmatrix} \quad \Sigma_2 = 2.3 \times \begin{bmatrix} 1 & 0.50 \\ 0.50 & 1 \end{bmatrix}$$

Visualisation of Test: variation of scale



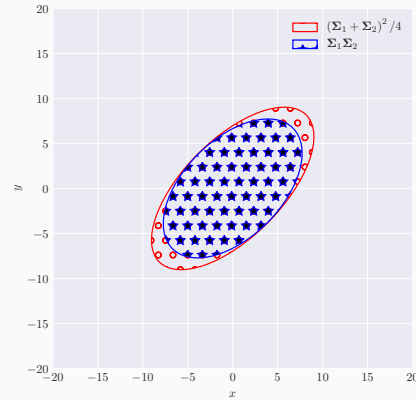
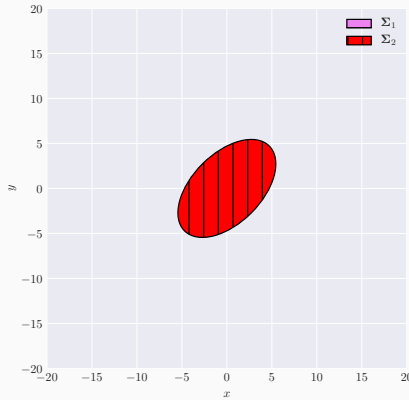
$$\Sigma_1 = \begin{bmatrix} 1 & 0.50 \\ 0.50 & 1 \end{bmatrix} \quad \Sigma_2 = 3.5 \times \begin{bmatrix} 1 & 0.50 \\ 0.50 & 1 \end{bmatrix}$$

Visualisation of Test: variation of scale



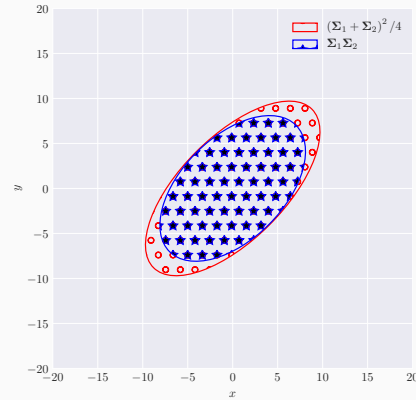
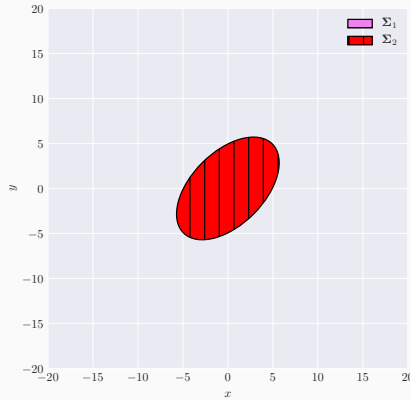
$$\Sigma_1 = \begin{bmatrix} 1 & 0.50 \\ 0.50 & 1 \end{bmatrix} \quad \Sigma_2 = 4.8 \times \begin{bmatrix} 1 & 0.50 \\ 0.50 & 1 \end{bmatrix}$$

Visualisation of Test: variation of scale



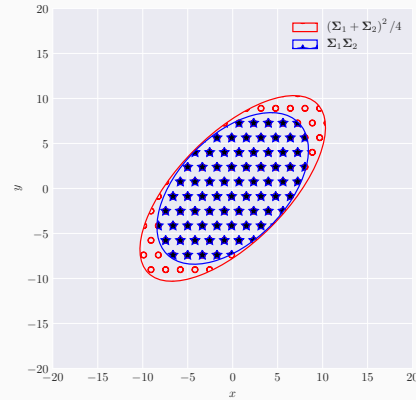
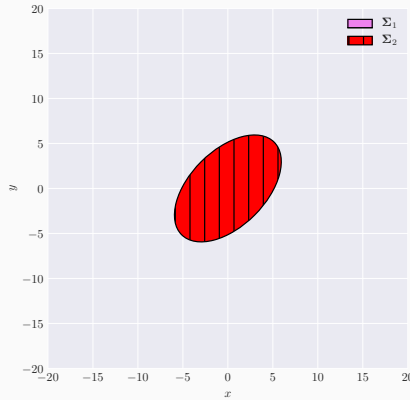
$$\Sigma_1 = \begin{bmatrix} 1 & 0.50 \\ 0.50 & 1 \end{bmatrix} \quad \Sigma_2 = 6.0 \times \begin{bmatrix} 1 & 0.50 \\ 0.50 & 1 \end{bmatrix}$$

Visualisation of Test: variation of scale



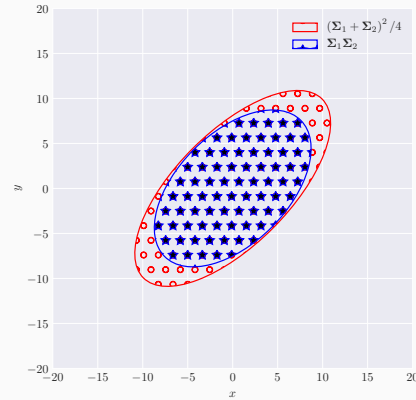
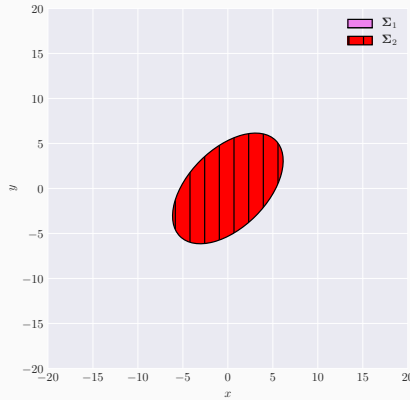
$$\Sigma_1 = \begin{bmatrix} 1 & 0.50 \\ 0.50 & 1 \end{bmatrix} \quad \Sigma_2 = 7.3 \times \begin{bmatrix} 1 & 0.50 \\ 0.50 & 1 \end{bmatrix}$$

Visualisation of Test: variation of scale



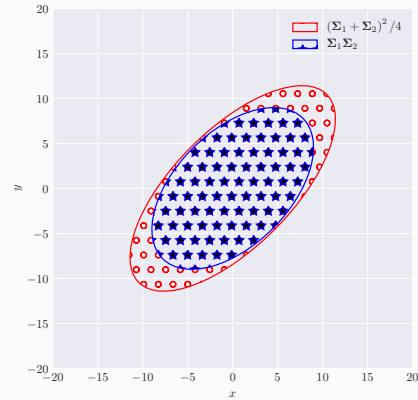
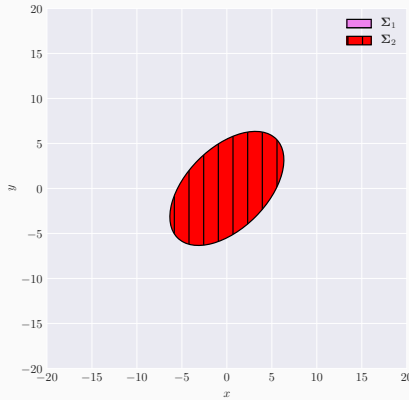
$$\Sigma_1 = \begin{bmatrix} 1 & 0.50 \\ 0.50 & 1 \end{bmatrix} \quad \Sigma_2 = 8.5 \times \begin{bmatrix} 1 & 0.50 \\ 0.50 & 1 \end{bmatrix}$$

Visualisation of Test: variation of scale



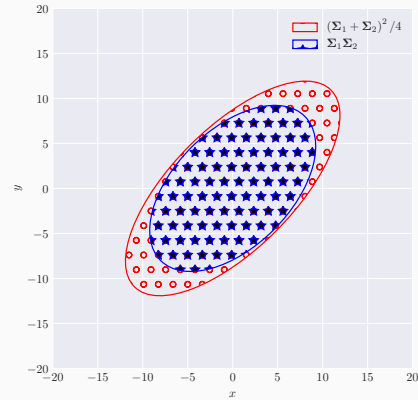
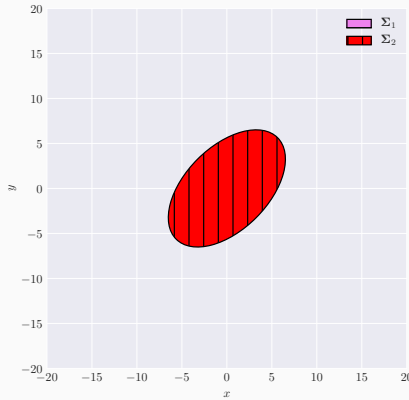
$$\Sigma_1 = \begin{bmatrix} 1 & 0.50 \\ 0.50 & 1 \end{bmatrix} \quad \Sigma_2 = 9.8 \times \begin{bmatrix} 1 & 0.50 \\ 0.50 & 1 \end{bmatrix}$$

Visualisation of Test: variation of scale



$$\Sigma_1 = \begin{bmatrix} 1 & 0.50 \\ 0.50 & 1 \end{bmatrix} \quad \Sigma_2 = 11.0 \times \begin{bmatrix} 1 & 0.50 \\ 0.50 & 1 \end{bmatrix}$$

Visualisation of Test: variation of scale



$$\Sigma_1 = \begin{bmatrix} 1 & 0.50 \\ 0.50 & 1 \end{bmatrix} \quad \Sigma_2 = 12.5 \times \begin{bmatrix} 1 & 0.50 \\ 0.50 & 1 \end{bmatrix}$$

Real Data Example: TropiSAR (1/2)

- Resolution of 1m
- Apparition of a vehicle in dense forest (Amazonian Forest)

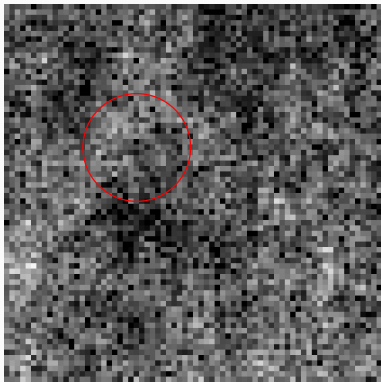
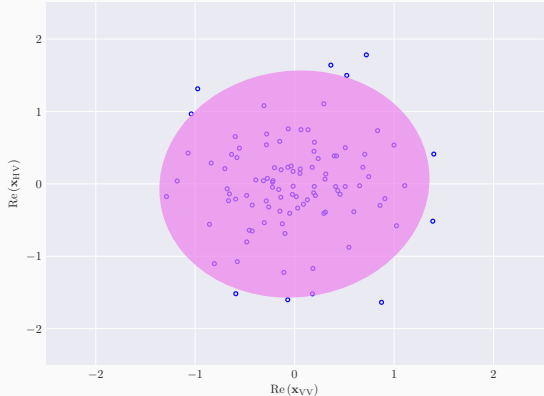


Image at t_1



Distribution of pixels inside circle at t_1

Real Data Example: TropiSAR (1/2)

- Resolution of 1m
- Apparition of a vehicle in dense forest (Amazonian Forest)

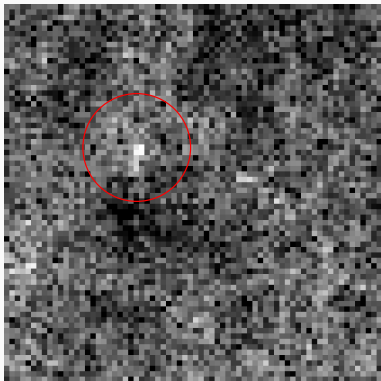
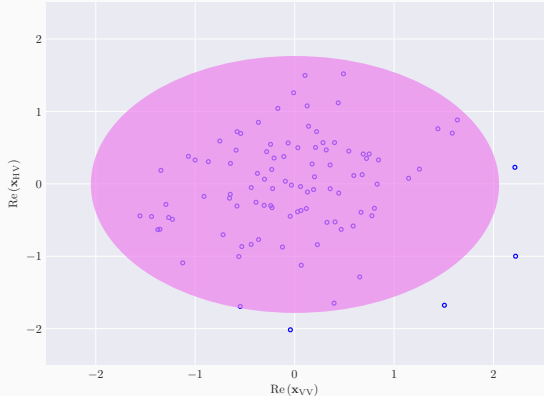
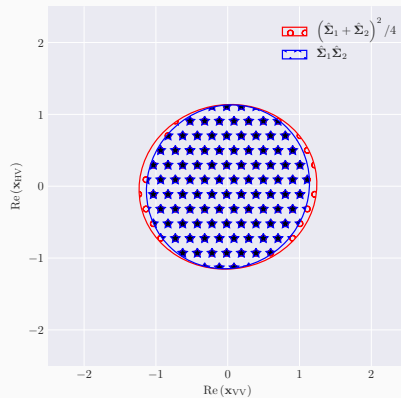
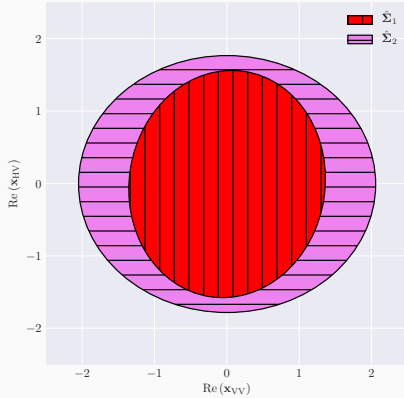


Image at t_2



Distribution of pixels inside circle at t_2

Real Data Example: TropiSAR (2/2)

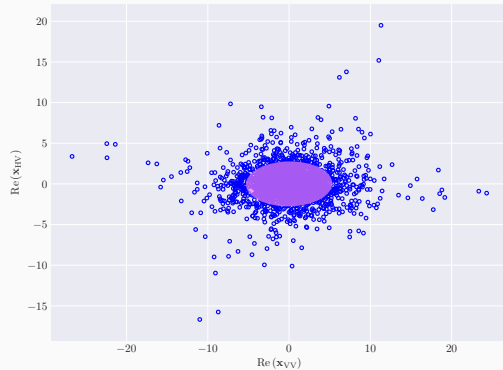
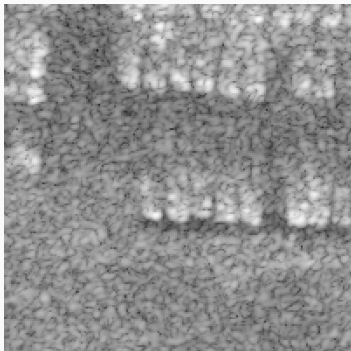


Change Detection in non-Gaussian Context

Non-Gaussian nature of SAR images (1/2)

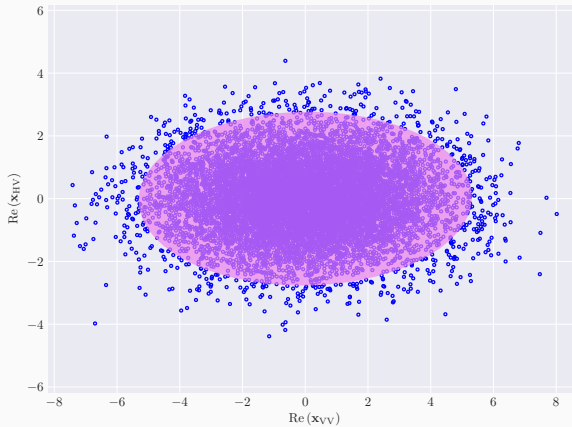
SDMS Dataset

- Available at <https://www.sdms.afrl.af.mil>
- Image FP0121 cropped at [2800:3000, 2000:2201]



Non-Gaussian nature of SAR images (2/2)

If the data was Gaussian:



SIRV modelling

To model this heterogeneous behaviour, a new family of distribution has been introduced: Spherically Invariant Random Vectors (SIRV) [Yao, 1973].

- Describes well the clutter in SAR images [Greco and Gini, 2007, E. et al., 2012]
- Model is given by:

$$\mathbf{x} \sim \sqrt{\tau} \mathbf{z} \text{ where } \mathbf{z} \sim \mathbb{C}\mathcal{N}(\mathbf{0}_p, \boldsymbol{\Sigma}) \text{ with } \text{Tr}\{\boldsymbol{\Sigma}\} = p$$

$p_\tau(\tau)$	$p_{\mathbf{x}}(\mathbf{x})$
$\delta(\tau_0)$	Gaussian
$\frac{b^2}{2} \exp(-\frac{b^2\tau}{2})$	Laplace
$\frac{b^2\tau^{-2}}{2} \exp(-\frac{b^2}{2\tau})$	Cauchy
$\left(\frac{b^2}{2}\right)^\nu \frac{\tau^{\nu-1}}{\Gamma(\nu)} \exp(-\frac{b^2\tau}{2})$	K-distribution
$\left(\frac{b^2}{2}\right)^\nu \frac{\tau^{\nu-1}}{\Gamma(\nu)} \exp(-\frac{b^2}{2\tau})$	Student-t

Illustration of SIRV

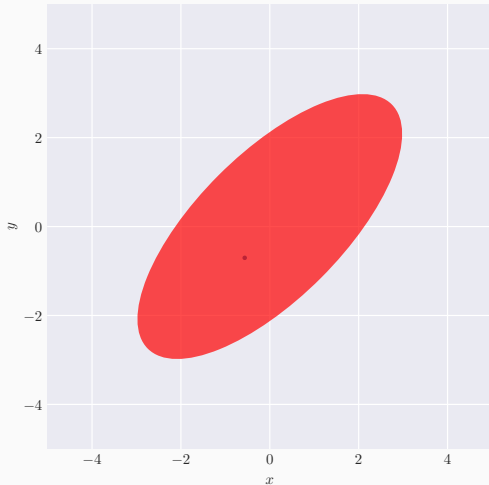
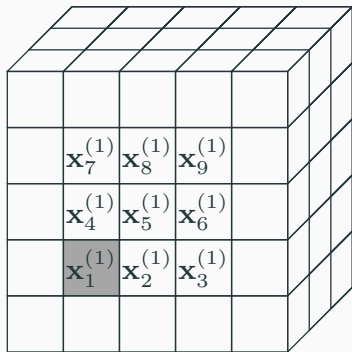


Illustration of SIRV

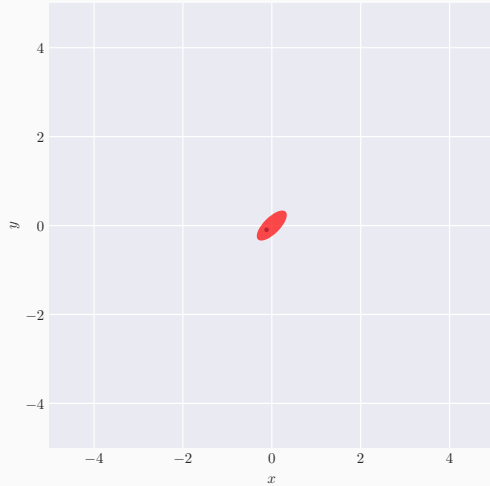
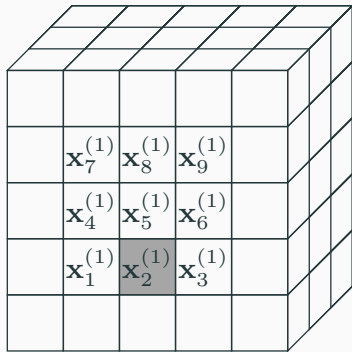
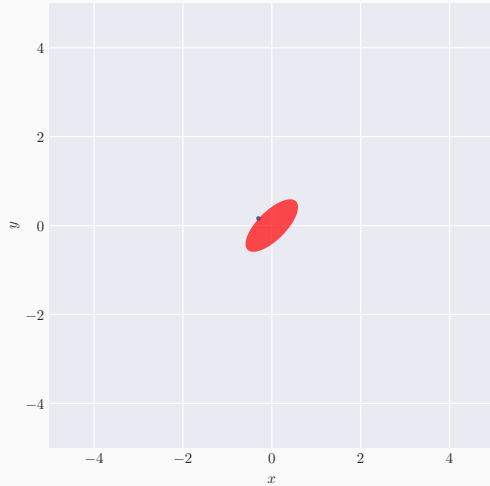
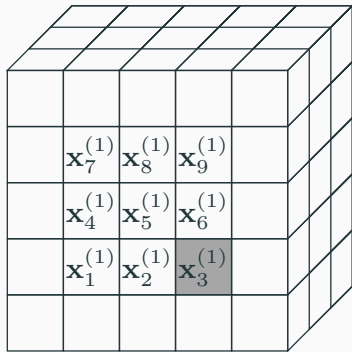


Illustration of SIRV



Change Detection under SIRV modelling

- To be independent of the type of distribution (while keeping the SIRV family), τ is considered as a **deterministic unknown** parameter: $\tau = \tau_k^{(t)}$.
- 3 problems of detection:

Problem 1:
 $\theta_t = \left\{ \tau_1^{(t)}, \dots, \tau_N^{(t)}, \Sigma_t \right\}$
 $\Phi_t = \{\emptyset\}$

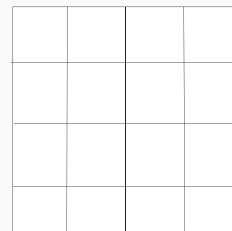
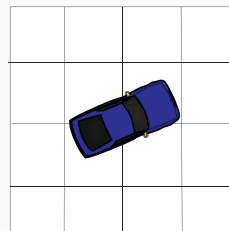
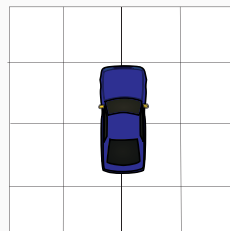
Scale and Shape

Problem 2:
 $\theta_t = \{\Sigma_t\}$
 $\Phi_t = \{\tau_1^{(t)}, \dots, \tau_N^{(t)}\}$

Shape

Problem 3:
 $\theta_t = \left\{ \tau_1^{(t)}, \dots, \tau_N^{(t)} \right\}$
 $\Phi_t = \{\Sigma_t\}$

Scale



Statistics of decision

- Use of Generalise Likelihood Ratio (GLRT) technique:

$$\hat{\Lambda} = \frac{\max_{\Omega_1, \dots, \Omega_T} \prod_{t=1}^T p_{\mathbf{x}_1^{(t)}, \dots, \mathbf{x}_N^{(t)}}(\mathbf{x}_1^{(t)}, \dots, \mathbf{x}_N^{(t)} / H_1; \boldsymbol{\Omega}_t)}{\max_{\Omega_0, \Phi_1, \dots, \Phi_T} \prod_{t=1}^T p_{\mathbf{x}_1^{(t)}, \dots, \mathbf{x}_N^{(t)}}(\mathbf{x}_1^{(t)}, \dots, \mathbf{x}_N^{(t)} / H_0; \boldsymbol{\theta}_0, \boldsymbol{\Phi}_t)} \stackrel{H_1}{\gtrless} \lambda.$$

- Technique known for good invariance properties [Kay and Gabriel, 2003]: useful to derive CFAR statistic.
- To simplify, we define:

$$q(\boldsymbol{\Sigma}, \mathbf{x}) = \mathbf{x}^H \boldsymbol{\Sigma}^{-1} \mathbf{x},$$

$$\forall k, \forall t, \mathbf{S}_k^{(t)} = \mathbf{x}_k^{(t)} \mathbf{x}_k^{(t)H}.$$

Statistics of decision for Problem 1 [Mian et al., 2018a]

The GLRT for Problem 1 yields:

$$\hat{\Lambda}_{\text{MT}} = \frac{\left| \hat{\Sigma}_0^{\text{MT}} \right|^{TN}}{\prod_{t=1}^T \left| \hat{\Sigma}_t^{\text{TE}} \right|^N} \prod_{k=1}^N \frac{\left(\sum_{t=1}^T q \left(\hat{\Sigma}_0^{\text{MT}}, \mathbf{x}_k^{(t)} \right) \right)^{Tp}}{T^{Tp} \prod_{t=1}^T \left(q \left(\hat{\Sigma}_t^{\text{TE}}, \mathbf{x}_k^{(t)} \right) \right)^p} \begin{matrix} \text{H}_1 \\ \gtrless \\ \text{H}_0 \end{matrix},$$

$$\hat{\Sigma}_t^{\text{TE}} = \frac{p}{N} \sum_{k=1}^N \frac{\mathbf{S}_k^{(t)}}{q \left(\hat{\Sigma}_t^{\text{TE}}, \mathbf{x}_k^{(t)} \right)}, \quad \hat{\Sigma}_0^{\text{MT}} = \frac{p}{N} \sum_{k=1}^N \frac{\sum_{t=1}^T \mathbf{S}_k^{(t)}}{\sum_{t=1}^T q \left(\hat{\Sigma}_0^{\text{MT}}, \mathbf{x}_k^{(t)} \right)}.$$

Statistics of decision for Problem 2 [Mian et al., 2018a]

The GLRT for Problem 2 yields:

$$\hat{\Lambda}_{\text{Mat}} = \frac{\left| \hat{\Sigma}_0^{\text{Mat}} \right|^{TN}}{\prod_{t=1}^T \left| \hat{\Sigma}_t^{\text{TE}} \right|^N} \prod_{k=1}^{k=N} \frac{\left(q \left(\hat{\Sigma}_0^{\text{Mat}}, \mathbf{x}_k^{(t)} \right) \right)^p}{\left(q \left(\hat{\Sigma}_t^{\text{TE}}, \mathbf{x}_k^{(t)} \right) \right)^p} \begin{matrix} \text{H}_1 \\ \gtrless \\ \text{H}_0 \end{matrix} \lambda,$$

$$\hat{\Sigma}_0^{\text{Mat}} = \frac{p}{TN} \sum_{t=1}^{t=T} \sum_{k=1}^{k=N} \frac{\mathbf{S}_k^{(t)}}{q \left(\hat{\Sigma}_0^{\text{Mat}}, \mathbf{x}_k^{(t)} \right)}.$$

Statistics of decision for Problem 3 [Mian et al., 2018a]

The GLRT for Problem 3 yields:

$$\hat{\Lambda}_{\text{Tex}} = \prod_{t=1}^T \frac{\left| \hat{\Sigma}_t^{\text{TE}} \right|}{\left| \hat{\Sigma}_t^{\text{Tex}} \right|} \prod_{k=1}^N \frac{\left(\sum_{t=1}^T q \left(\hat{\Sigma}_t^{\text{Tex}}, \mathbf{x}_k^{(t)} \right) \right)^{Tp}}{T^{Tp} \prod_{t=1}^T \left(q \left(\hat{\Sigma}_t^{\text{TE}}, \mathbf{x}_k^{(t)} \right) \right)^p} \stackrel{\text{H}_1}{\gtrless} \lambda, \stackrel{\text{H}_0}{\lessgtr}$$

$$\hat{\Sigma}_t^{\text{Tex}} = \frac{Tp}{N} \sum_{k=1}^N \frac{\mathbf{s}_k^{(t)}}{\sum_{t'=1}^T q \left(\hat{\Sigma}_t^{\text{Tex}}, \mathbf{x}_k^{(t)} \right)}.$$

Properties

Proposition

- $\hat{\Lambda}_{\text{MT}}$, $\hat{\Lambda}_{\text{Mat}}$, $\hat{\Lambda}_{\text{Tex}}$ are CFAR texture.
- $\hat{\Lambda}_{\text{MT}}$ and $\hat{\Lambda}_{\text{Mat}}$ are CFAR matrix.
- $\hat{\Lambda}_{\text{Tex}}$ is not CFAR matrix.

Sketch of the proof:

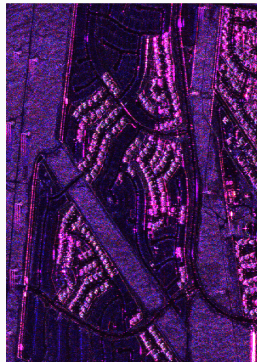
- Texture: For any set $\{\tau_k^{(t)} / (k, t) \in [\![1, N]\!] \times [\![1, T]\!]\}$ under H_0 assumption, the statistic are invariant by the substitution $\mathbf{x}_k^{(t)} \rightarrow \mathbf{x}_k^{(t)} / \tau_k^{(t)}$.
- Matrix: $\hat{\Lambda}_{\text{MT}}$ and $\hat{\Lambda}_{\text{Mat}}$ are invariant for the group of transformation

$$\mathcal{G} = \left\{ \mathbf{G} \mathbf{x}_k^{(t)} / t \in [\![1, T]\!], k \in [\![1, N]\!], \mathbf{G} \in \mathbb{S}_{\mathbb{H}}^p \right\}.$$

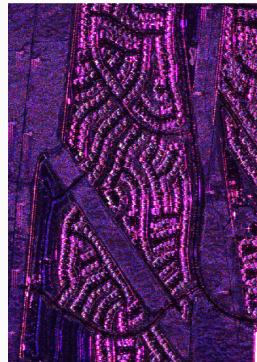
For $\hat{\Lambda}_{\text{Tex}}$, the trace normalisation gives it a non-CFAR behaviour at finite distance.

Example on UAVSAR (NASA) dataset

- Polarimetric data: $p = 3$
- Dimensions: 2360px 600px
- Resolution: 1.67 m (Range) and 0.60 m (Azimuth)



April 23, 2009



May 1, 2011



Example on UAVSAR (NASA) dataset ($p = 3, N = 81$)

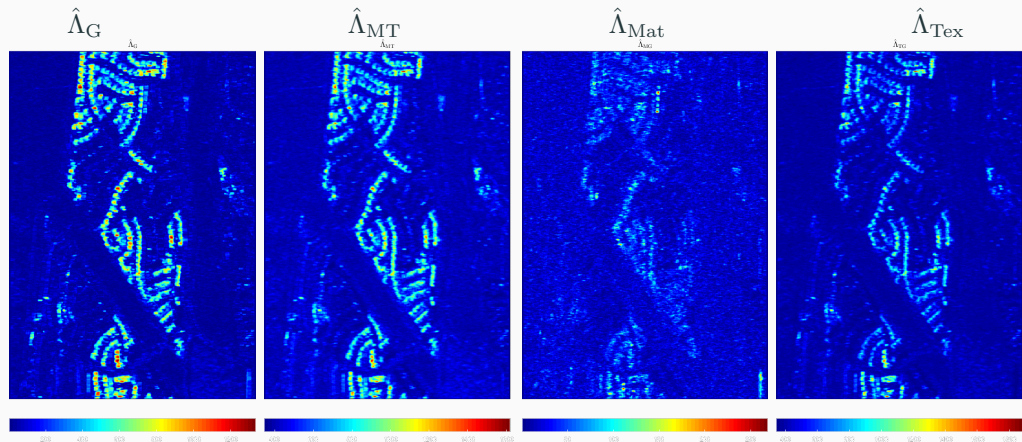
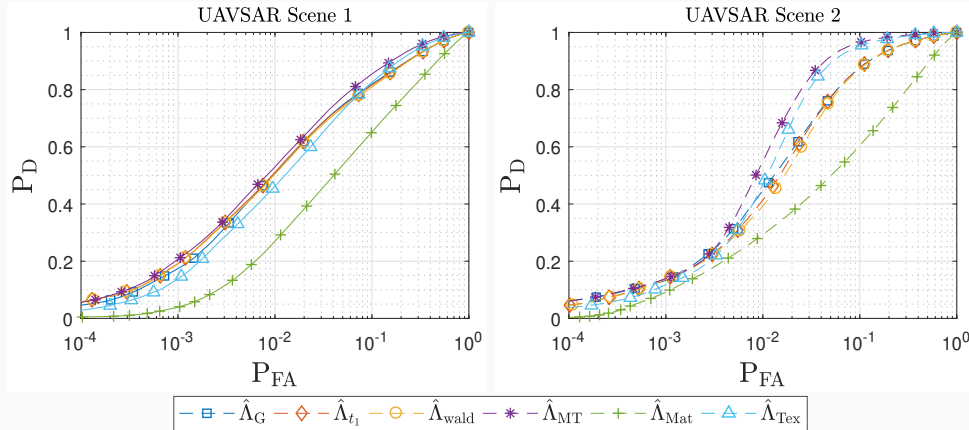


Figure 1: Values of log of statistics

Example on UAVSAR (NASA) dataset ($p = 3$, $N = 121$)



Example of SDMS Time Series



Example of SDMS Time Series



Example of SDMS Time Series



Example of SDMS Time Series



Example of SDMS Time Series



Example of SDMS Time Series



Example of SDMS Time Series



Example of SDMS Time Series



Example of SDMS Time Series

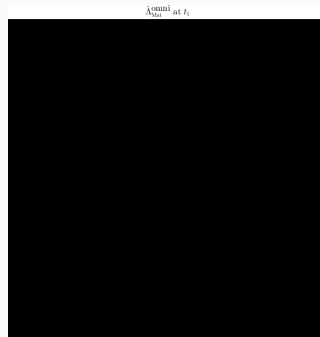
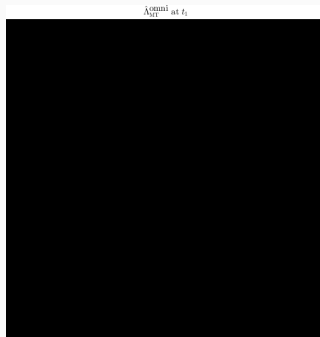
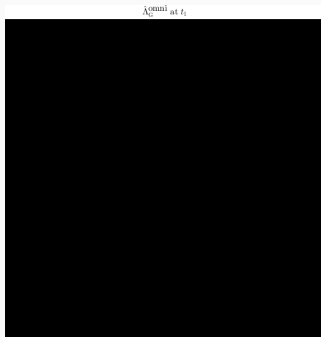


Example of SDMS Time Series

Image at t_{10}



Example of SDMS Time Series: Results



Example of SDMS Time Series: Results



Example of SDMS Time Series: Results



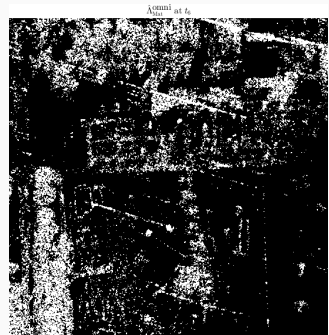
Example of SDMS Time Series: Results



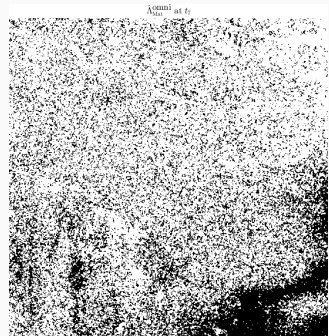
Example of SDMS Time Series: Results



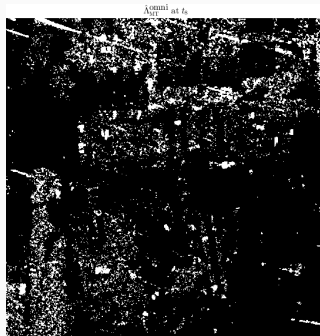
Example of SDMS Time Series: Results



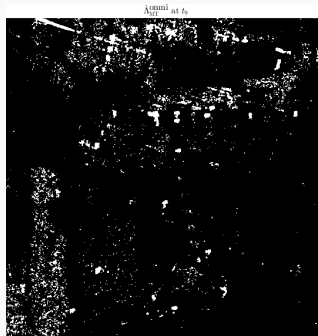
Example of SDMS Time Series: Results



Example of SDMS Time Series: Results



Example of SDMS Time Series: Results



Example of SDMS Time Series: Results



Conclusions

- New methods for change detection and change-point estimation have been developed.
- Highlighted that texture parameter is important when modelling changes.
- Robust statistics deal better with false alarm regulation and have better performance of detection.
- Perspectives:
 - Derive theoretical performance of new statistics (Distribution under H_0).
 - Classification of Changes in time series (Spatio-temporal clustering).

References i

-  Ciuonzo, D., Carotenuto, V., and Maio, A. D. (2017).
On multiple covariance equality testing with application to SAR change detection.
IEEE Transactions on Signal Processing, 65(19):5078–5091.
-  Conradsen, K., Nielsen, A. A., Schou, J., and Skriver, H. (2001).
Change detection in polarimetric SAR data and the complex Wishart distribution.
In *IGARSS 2001. Scanning the Present and Resolving the Future. Proceedings. IEEE 2001 International Geoscience and Remote Sensing Symposium (Cat. No.01CH37217)*, volume 6, pages 2628–2630 vol.6.

-  E., Tyler, D. E., Koivunen, V., and Poor, H. V. (2012).
Compound-Gaussian clutter modeling with an inverse Gaussian texture distribution.
IEEE Signal Processing Letters, 19(12):876–879.
-  Greco, M. S. and Gini, F. (2007).
Statistical analysis of high-resolution SAR ground clutter data.
IEEE Transactions on Geoscience and Remote Sensing, 45(3):566–575.
-  Hussain, M., Chen, D., Cheng, A., Wei, H., and Stanley, D. (2013).
Change detection from remotely sensed images: From pixel-based to object-based approaches.
{ISPRS} Journal of Photogrammetry and Remote Sensing, 80:91 – 106.

-  Kay, S. M. and Gabriel, J. R. (2003).
An invariance property of the generalized likelihood ratio test.
IEEE Signal processing letters, 10(12):352–355.
-  Mian, A., Ovarlez, J. P., Ginolhac, G., and Atto, A. (2017).
2017 25th european signal processing conference (eusipco).
In *Multivariate change detection on high resolution monovariate SAR image using linear time-frequency analysis*, pages 1942–1946.
-  Mian, A., Ovarlez, J.-P., Ginolhac, G., and Atto, A. M. (2018a).
New robust statistics for change detection in an image time series of multivariate sar images.
Transactions on Signal Processing.

-  Mian, A., Ovarlez, J.-P., Ginolhac, G., and Atto, A. M. (2018b).
New wavelet packet adapted to high-resolution sar images analysis with an application to robust target detection.
Transactions on Geoscience and Remote Sensing.
-  Nascimento, A. D. C., Frery, A. C., and Cintra, R. J. (2018).
Detecting Changes in Fully Polarimetric SAR Imagery with Statistical Information Theory.
ArXiv e-prints.
-  Novak, L. M. (2005a).
Change detection for multi-polarization multi-pass sar.
In *Defense and Security*, pages 234–246. International Society for Optics and Photonics.

-  Novak, L. M. (2005b).
Coherent change detection for multi-polarization sar.
In *Conference Record of the Thirty-Ninth Asilomar Conference on Signals, Systems and Computers, 2005.*, pages 568–573.
-  Preiss, M. and Stacy, N. J. S. (2008).
Polarimetric sar coherent change detection.
In *7th European Conference on Synthetic Aperture Radar*, pages 1–4.
-  Ratha, D., De, S., Celik, T., and Bhattacharya, A. (2017).
Change detection in polarimetric SAR images using a geodesic distance between scattering mechanisms.
IEEE Geoscience and Remote Sensing Letters, 14(7):1066–1070.

-  Yao, K. (1973).
A Representation Theorem and its Applications to Spherically Invariant Random Processes.
Information Theory, IEEE Transactions on, 19:600–608.